33rd Annual International Conference of the IEEE EMBS
Boston, Massachusetts USA, August 30 - September 3, 2011

MEMS-Based Bubble Pressure Sensor for Prosthetic Socket Interface Pressure Measurement

Jason W. Wheeler, Jeffrey G. Dabling, Douglas Chinn, Timothy Turner, Anton Filatov, Larry Anderson and Brandon Rohrer

Abstract— **The ability to chronically monitor pressure at the prosthetic socket/residual limb interface could provide important data to the research and clinical communities. With this application in mind, we describe a novel type of sensor which consists of a MEMS pressure sensor and custom electronics packaged in a fluid-filled bubble. The sensor is characterized and compared to two commercially-available technologies. The bubble sensor has excellent drift performance and good sensing resolution. It exhibits hysteresis which may be due to the silicone that the sensor is molded in. To reduce hysteresis, it may be advisable to place the sensor between the liner and the socket rather molding directly into the liner.**

I. Introduction

Maintainance of a quality socket fit is one of the most important issues for amputees and prosthetists [1]. The prosthetist often attempts to distribute interface pressures across the residual limb such that there is contact everywhere but load-tolerant areas support larger pressures. Bony-prominences, such as the anterior tibia in below-knee prostheses are generally considered to be relatively load-intolerant areas and pressure is often diverted to surrounding soft-tissue areas by making reductions on the residual limb model [2].

The prosthetist's task of creating the desired fit is made more difficult because the shape and volume of the residual limb vary over time. As the amputee walks, fluid is pumped out of the residual limb and it generally loses volume. This volume loss is not spatially uniform as soft-tissue areas lose more volume than bony areas [3,4]. Measurement of socket-limb interface pressures can provide information about the fit quality as these volume changes occur which is of interest to researchers and clinicians. Additionally, an active variable-volume socket that can make local adjustments to accommodate volume fluctuations would require chronic pressure measurement.

Several systems have been used to measure socket interface pressures. The most common approach is to use force sensitive resistor (FSR) technology. These sensors are quite thin and can be arranged with a high spatial resolution in the socket. Their sensing performance is severely limited due to several factors; most notably non-linearity, hysteresis and drift [5,6] and they are not typically relied on to provide reliable absolute pressure measurements. Sanders et al. used high performance, three-axis force sensors to provide high-fidelity measurements at a lower spatial resolution [7]. This system was designed for biomechanical research and is not well suited for chronic use in a clinical setting.

In this paper we present a novel sensor for chronic monitoring of prosthetic socket interface pressures. The sensor consists of a commercial MEMS pressure sensor that is mounted with electronics in a custom ceramic package and molded into a fluid-filled bubble. The sensor is designed to be placed between the socket and the liner or molded directly into a liner. We first present the design and fabrication of the sensor, followed by a characterization and comparison to commercial technology.

II. Sensor Design and Fabrication

This section describes the sensor design, components and fabrication methods. The sensor consists of a commercial unpackaged MEMS pressure sensor which is mounted in a custom ceramic package (shoebox). This shoebox is then embedded in a fluid-filled silicone bubble.

A. MEMS Sensor Packaging

The pressure transducer shoebox package was fabricated using six layers of Low Temperature Co-fired Ceramic (LTCC). The various layers were punched from 0.25mm thick DuPont 951® green tape. Conductor traces were printed on the two floor layers using DuPont 5734 gold thick film conductor paste and interconnected through vias. The cavity was formed using three layers of 10 mil green tape (see Figure 1). The five layers were assembled on a pinned 7.6x7.6 cm steel lamination fixture, covered with the rubber mold, vacuum bagged and laminated for 15 minutes at 20.7 MPa and 67°C. Cavity walls were protected from deformation during lamination by using a mold made from Dow Corning Silastic J RTV Silicone Rubber. Each fixture yields six packages. The laminated lid layers were then fired at 850°C in a belt furnace.

After singulation, the individual packages were populated with an Endevco (San Juan Capistrano, CA) model 32394 silicon MEMS pressure transducer, an unpackaged amplifier (LT1789-10) and a capacitor. The pressure transducer and capacitor were attached using Ablebond 8175A silver epoxy and the amplifier was attached using Ablebond JM7000NC non-conductive epoxy. The epoxy was cured for 30 minutes

Manuscript received March 26, 2011. This work was supported in part by the U.S. Army Telemedicine and Advanced Technology Research Center and the Congressionally Directed Medical Research Program.

The authors are with Sandia National Laboratories, Albuquerque, NM 87185 USA (e-mail: jwwheel@sandia.gov).

at 150°C. The amplifier was wire bonded to the package floor traces and then covered with Ablebond JM7900 glob top to provide mechanical protection for the bonds and amplifier. The lid layer was attached to the package body using Ablebond JM7000NC epoxy and cured for 30 minutes. 15.4 cm long 30 ga. stranded wire leads were attached to the bond pads on the left (Figure 1) using Ablebond 8175A silver epoxy, then encapsulated at the attachment points using Hardman 5 minute epoxy to provide strain relief. The final shoebox dimensions were 6.4x4.6x1.3 mm.

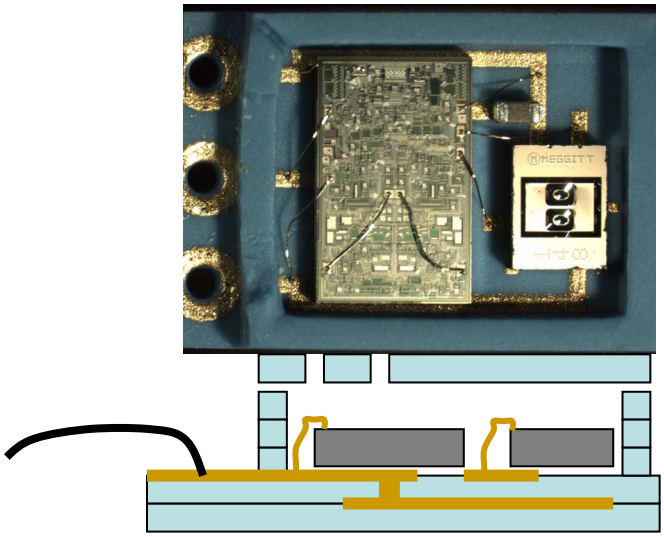

Fig. 1. Sensor bonded to electronics inside package (top) with side view schematic (bottom).

B. Bubble Fabrication

The manufacturing method discussed here describes how the shoebox assembly was enveloped in a pool of silicone fluid encapsulated in a bubble.

A 0.25mm thick layer of silicone film was fitted over the concave cavities of two plungers, shown in Fig. 2 (left panel), and held in place by two oval rings that snap over the external lip of the cavity. The plunger has a small air channel leading from the center of the cavity to a septum on the back of the plunger. The silicone film was stretched to conform to the cavity by removing the air in the septum with a syringe.

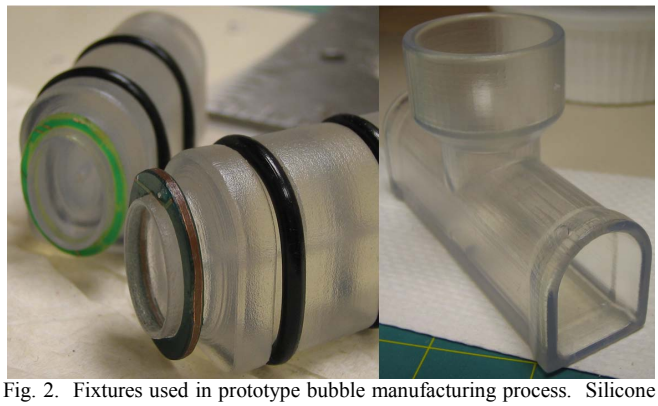

Fig. 2. Fixtures used in prototype bubble manufacturing process. Silicone film is stretched onto the plungers on the left. After some processing, the plungers are then inserted into the side cavities of the housing fixture shown on the right.

With the silicone film held in place under slight vacuum, a thin bead of silicone adhesive (RTV) was applied to the rim of the bubble cavity, and the plungers were inserted into the opposite ends of the housing shown in the right panel of Figure 2. The top cavity of the fixture was then filled with 350 centistoke silicone fluid, which surrounded the film-covered plunger cavities. The o-rings surrounding the plungers prevented the fluid from leaking out the other openings in the fixture. The wired shoebox assembly was lowered into the silicone fluid such that it was centered between the two plunger cavities. The plungers were then simultaneously compressed until the two cavity halves were closed around the shoebox, the silicone adhesive creating a tight seal between the cavity halves and around the shoebox wires.

After sufficient adhesive cure time, the snap rings were removed from the plungers, the plungers pulled out of the fixture and the bubble was complete, as shown in **Error! Reference source not found.**. The primary axes of the bubble measured approximately 16x9x5 mm.

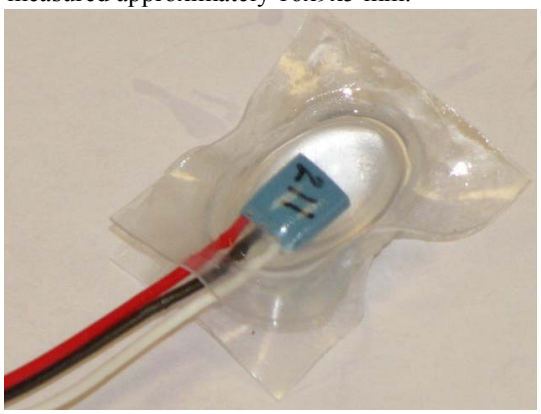

Fig. 3. Bubble sensor in final packaged form. Excess material can be trimmed around the sealed region.

In the studies described in this paper, the bubble was molded into a 7mm layer of 20 shore A silicone rubber. This allowed a more uniform load to be applied for characterization. This embodiment resembled molding the bubbles directly into a prosthetic liner.

III. Sensor Characterization

The sensor described above was tested on a flat surface to characterize its performance in conditions resembling those in the proposed application. For comparison, two commercially available sensors were also tested in the same manner: The Tekscan (South Boston, MA) Flexiforce A401-25 FSR and the Pressure Profiles (Los Angeles, CA) C500 capacitive sensor. The tests described here were used to calibrate the sensors and characterize drift and hysteresis.

A. Test hardware and methods

Signals from the commercial sensors were conditioned using circuitry recommended by the manufacturer. Pressure Profiles provides this circuitry integrated with their product, while the Flexiforce sensor was operated using a simple

filter/amplifier circuit recommended by Tekscan, with a gain chosen to optimize performance over the pressure range of interest.

Most sensor characterization was performed by applying loads to the sensors via an MTS (Eden Prairie, MN) Alliance RT/5 electromechanical load frame outfitted with a calibrated 5kN load cell. Loads of various profiles were applied to the sensors, which enabled comparison of the sensor output (voltage) to the MTS load cell output (force). Sensor outputs were recorded and synchronized by inputting data from the circuits through an analog-to-serial convertor to the MTS machine at 10 Hz.

In order to create a nearly uniform pressure over the surface of the sensors, loads were applied through a thin (5mm) layer or 20 shore A silicone. For the bubble sensor and FSR, a 2.5 inch diameter aluminum disk was used as the applicator and the silicone layer was cut to the same size and shape. The bubble sensor, when molded in silicone, was flat, so a uniform pressure was easy to achieve. The FSR was smaller than the disk but was thin enough (0.2mm) that the pressure was generally uniform across the sensor surface. The capacitive sensor was somewhat thicker so a custom applicator and piece of silicone were made that were the same size and shape as the sensor.

To calibrate the sensors and characterize hysteresis, a stair-step pattern of loads was applied. Thirteen equally spaced loads were applied in increasing order up to a maximum pressure of 182 kPa. The same loads were then applied in decreasing order. The silicone introduced some creep into the force data, so the position of the MTS machine was held at a fixed position for about one minute after the desired load was reached.

Drift characterization was performed by placing an 85 lb dead weight on the sensor (through the silicone as in the MTS tests) and recording data at 100 Hz for 1 hour.

B. Data Analysis

As describe above, the silicone introduced some creep into the force measured by the MTS load cell at a given position. The machine was not capable of doing direct force control to compensate for this. We therefore held the position once the desired force was reached for about one minute. After recording the data, we selected 100 points (10 seconds) of data after any transients in the load cell readings had settled. Only these points were considered in the data analysis.

To characterize the sensing performance, the sensor outputs were plotted versus the load cell force and a 5th order polynomial was fit to the data. Only the load applied during the increasing portion of the test was considered in this part of the analysis. The norm of the residuals was calculated for the polynomial fits to provide a measure of fit quality.

Hysteresis was evaluated by plotting sensor data versus load cell data for both the increasing and decreasing portions of the tests.

For the drift tests, the sensor outputs were calibrated using the polynomial fit chosen in the previous analysis. The data were then low-pass filtered (5th order Butterworth with a cutoff of 0.2 Hz) and plotted versus time.

IV. Results

The calibration data for the sensors are shown in Figure 4 along with the polynomial fits. The norm of residuals was lowest for the capacitive sensor (22.3) and was larger for the bubble and FSR (79.2 and 68.4 respectively). Higher order fits did not substantially decrease the norm of residuals.

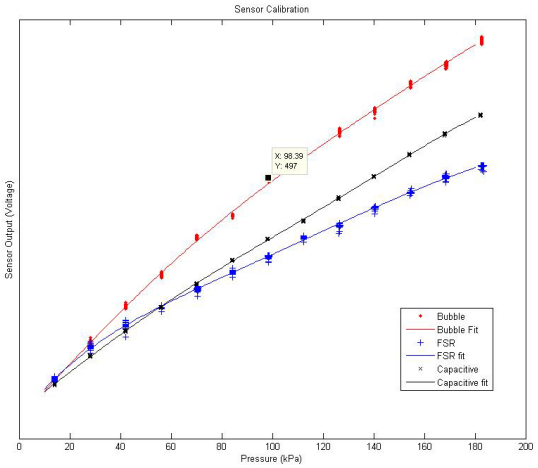

Fig. 4. Calibration data for each of the three sensors along with 5th order polynomial fit. Vertical axis is a linear scale of sensor output voltage which was shifted (but not scaled) to facilitate comparison.

Hysteresis plots for the three sensors are shown in Figure 5. The bubble sensor had the largest hysteresis, which may be attributable to the silicone material that it is molded and packaged in as discussed in the Conclusions below.

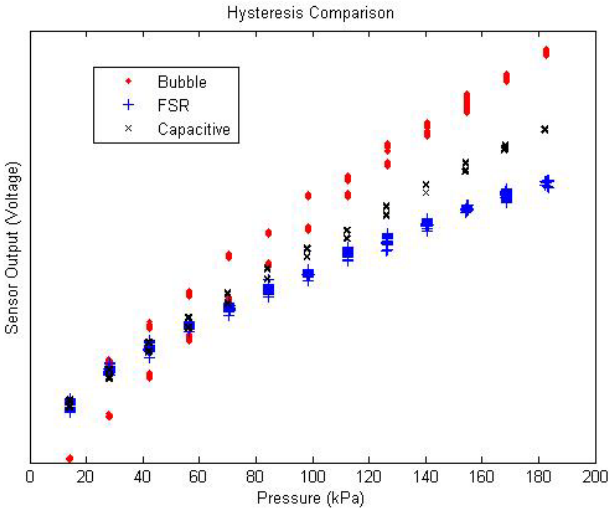

Fig. 5. Hysteresis plots for the three sensors. Vertical axis is a linear scale of sensor output voltage which was shifted (but not scaled) to facilitate comparison.

Drift data are presented in Figure 6. The capacitive sensor and FSR signals exhibit substantial drift over the first several minutes and are still drifting after one hour. The capacitive sensor exhibits the most drift in this case. The bubble sensor drifts very little over the test.

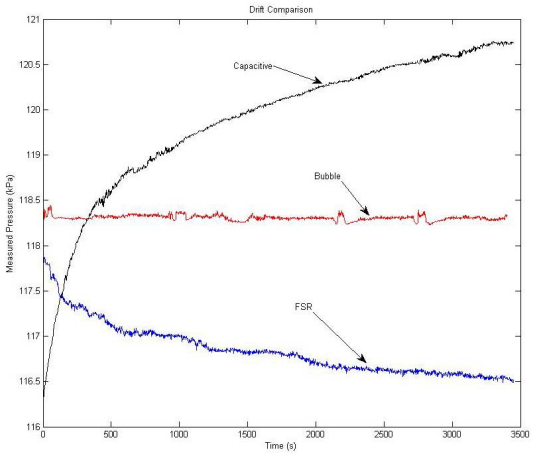

Fig. 6. Drift data over one hour for the three sensors.

V. CONCLUSION

The bubble sensor described in the present work had reasonable sensing performance over the pressure range of interest (prosthetic socket interface pressures are generally less than about 180 kPa). When compared to the two commercial sensors, the bubble sensor had excellent drift characteristics. Drift is critical for this application (and many others) because it is very difficult to compensate or calibrate for.

The bubble sensor did exhibit substantial hysteresis compared to the commercial technologies. This is problematic for the intended application though it may be possible to calibrate for. We hypothesized that much of the hysteresis seen in these tests was due to the silicone material that the bubble was molded and packaged in. Because the sensor has non-negligible thickness, it is likely not completely in series with the silicone layers. It is therefore possible that the sensor could adopt some of the hysteretic behavior of the surrounding material. To test this, loads were manually applied to an isolated bubble (not molded in silicone) which was placed in series with the capacitive sensor used in the previous tests (which exhibited very little hysteresis). The results are shown in Figure 7.

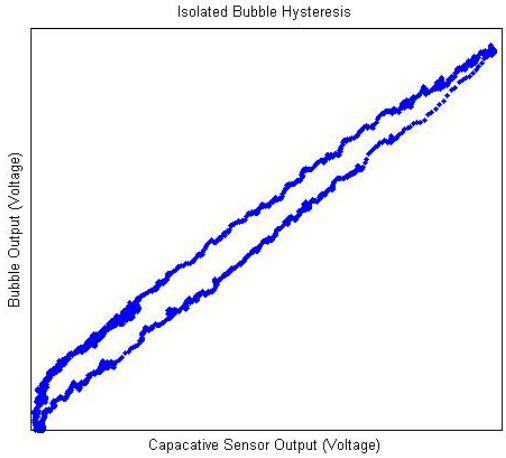

Fig. 7. Plot of the isolated bubble output versus series capacitive sensor output. Hysteresis is reduced compared to data in Figure 5 but is still significant.

The hysteresis was reduced in the configuration but is still present (approximately 10% of full-scale reading). The remaining effect is likely due to the silicone sheets used to package the bubble. Other materials will be tested to see if the effect can be reduced. Based on these findings, it may be better not to mold a sensor of non-negligible thickness directly into a liner material (all of which are likely to be hysteretic to varying degrees). We are currently developing other packaging methods that may mitigate these effects.

Overall, the capacitive sensor showed the best sensing performance in terms of linearity, resolution and hysteresis but had the largest signal drift. From a practical point of view, the capacitive sensor may not be ideal for this application due to the cost and relative complexity of electronics. The FSR showed reasonable sensing performance in this test in terms of hysteresis and resolution but the signal drift was significant. These sensors are very inexpensive and do not require complex electronics, which had led to their popularity for this and other applications. As previously documented (and also found in this study) however, their performance has fundamental limitations [5-6]. The bubble sensor appears to have substantial advantages in drift performance but more work is needed to address hysteresis. Practically, the bubble electronics are included in the sensor so the signal conditioning requirements are minimal, which should facilitate scaling to several sensors. The fabrication process described here was intended for small batches and a more refined process would be needed to bring the cost down for mass production.

ACKNOWLEDGMENT

The authors would like to thank Curt Salisbury for assistance with the current work.

REFERENCES

[1] M. Legro, G. Reiber, M. del Aguila, M., Ajax, D. Boone, J. Larson, D. Smith, and B. Sangeorzan, "Issues of importance reported by persons with lower-limb amputations and prostheses." *J. Rehab. Res. and Dev.*, vol. 36, no. 3. 1999.

[2] G. M. Berke, "Transtibial Prosthetics," in *Orthotics and Prosthetics in Rehabilitation*, M. Lusardi, C. Nielson, Eds. Butterworth Heinemann, 2000, pp. 437-466.

[3] J. Sanders, S. Zachariah, A. Jacobsen, and J. Fergason, "Changes in interface pressures and shear stresses over time on trans-tibail amputee subjects ambulating with prosthetic limbs: comparison of diurnal and six-month differences," *J. Biomechanics,* vol. 38, no. 8, pp. 1566-1573, 2005.

[4] J. Sanders, "Stump-socket interface conditions," in *Pressure Ulcer Research: Current and Future Persepctives*, D. Bader, C. Bouten, C. Oomens Eds, Springer, 2006, pp. 129-147.

[5] A. Buis, and P. Covery, "Calibration problems encountered while monitoring stump/socket interface pressures with force sensing resistors: techniques adopted to minimize inaccuracies," *Prosth. And Orhtot. Int.,* vol. 21, pp. 179-182, 1997.

[6] A. Hollinger, and M. Wanderley, "Evaluation of Commercial Force-Sensing Resistors," in 2006 *Proc. New Interfaces for Mus. Express.,* Paris, 2006.

[7] J. Sanders, D. Lam, A. Dralle, and R. Okamura, "Interface pressures and shear stresses at thirteen socket sites on two persons with transtibial amputation," in *J. Rehab. Res.,* vol. 34, no. 1, pp. 19-43, 1997.